Journal of Polymers and the Environment (2018) 26:2917–2924
https://doi.org/10.1007/s10924-017-1171-6

ORIGINAL PAPER

Preparation, Characterization and Dye Adsorption/Reuse of Chitosan-Vanadate Films

Denys A. S. Rodrigues[1] · Jaqueline M. Moura[1] · Guilherme L. Dotto[2] · Tito R. S. Cadaval Jr.[1] · Luiz A. A. Pinto[1]

Published online: 24 January 2018

Abstract

Chitosan used on dyes adsorption when in film form shows limitations due to its low regeneration capacity. In this work, chitosan films were modified using vanadium ions to improve its regeneration capacity on the dye adsorption. Films were characterized and analyzed by FT-IR, XRD and DSC. Adsorption assays were performed using chitosan-vanadate films (CVF) to remove the Reactive Black 5 dye in aqueous solution. The adsorption was favored by the pH decrease from 8.0 to 4.0. The equilibrium data were best fitted by Langmuir model, with q_m of 522 mg g^{-1} at 298 K. The negative value of ΔH^0 (−9.91 kJ mol^{-1}) showed an exothermic operation and the value of ΔS^0 was positive (0.0705 kJ mol^{-1} K^{-1}), suggesting an increase in randomness at the solid/solution interface. The kinetics was represented by pseudo-first order model and around 80 min occurred a reduction in the adsorption rates, due to the mass transfer mechanism. The most appropriate eluent to remove the RB5 from CVF was NH_4OH 0.01 kg mol L^{-1}. The CVF used to the dye adsorption were regenerated and reutilized five times, and the adsorption capacity was around 80% of the initial value after the last cycle.

Keywords Dye adsorption · Equilibrium · Film · Kinetics · Polymers · Wastewater treatment

Introduction

Synthetic dyes are present in the wastewater of different industries, such as textiles, paper, plastics and foods [1–4]. The presence of these molecules in aquifers changes the water color and reduces the oxygen solubility, impacting in the photosynthetic metabolism of aquatic plants [5]. Reactive Black 5 (RB5) anionic dye is one of the most used in textile industries, as well as, it is one of the most toxic [6]. Many techniques have been used to effluents treatment containing dye, such as, oxidation, coagulation/flocculation, electrochemical coagulation, biological treatment and ion-exchange resins, however, these are not economically viable in processes of low dyes concentrations [7]. The adsorption operation is one of the most convenient and low-cost alternatives for the removal of contaminants from aqueous solutions [8–14].

Several alternative adsorbents have been employed to remove dyes from aqueous solutions. Chitosan-based materials stand out due to its high contents of amino and hydroxyl groups, which present high potential for interaction with the contaminants [5]. Chitosan can be isolated from marine chitin [15–20]. Among the chitosan based materials, the chitosan film (CF) is an interesting shape to remove contaminants from aqueous solutions [21]. The main advantages for the application of chitosan film are its good tensile strength, elongation, swelling properties, applicability to a large pH range and its easy separation from the solution after adsorption [22].

However, in the adsorption operation using CF as adsorbent, the desorption and the reuse of the films are key factors from the economical viewpoint [23]. In this way, it is necessary to perform studies about possible changes in the CF, which could to enable a higher number of adsorption–desorption cycles, keeping their adsorption capacities similar to the pure film. Cadaval Jr et al. [24] studied the removal of vanadium ions in aqueous solutions using CF as adsorbent, and the authors reported that the films were used by six cycles, being maintained the its physical characteristics

✉ Luiz A. A. Pinto
dqmpinto@furg.br

[1] School of Chemistry and Food, Federal University of Rio Grande–FURG, km 8, Italia Avenue, Rio Grande, RS 96203900, Brazil

[2] Environmental Processes Laboratory, Chemical Engineering Department, Federal University of Santa Maria–UFSM, 1000, Roraima Avenue, Santa Maria, RS 97105–900, Brazil

and the adsorption capacity. This reuse capacity suggests that, the vanadium ions led to modification the interactions between the polymer chains and, consequently, caused the morphological and structural changes, which enabled to reuse of the films. Based on these results, it is interesting to investigate this modification in CF and the alterations occurred in the polymeric structure due to the interaction with the vanadate ions, as well as, evaluate it in the adsorption and reuse.

Thus, this study was aimed to modify the CF using vanadium ions to improve its regeneration capacity in the dyes adsorption. CF were prepared by casting technique, and the films were modified using vanadium salt, afterwards, the elution assays to remove the ions were performed. The modified CF with vanadium ions were analyzed by mechanical characteristics, Fourier transform infrared spectroscopy, X-ray diffraction and differential scanning calorimetry. Finally, the RB5 adsorption onto chitosan-vanadate films (CVF) was investigated by the kinetics, equilibrium and thermodynamic, as also, by the film reuse.

Materials and Methods

Reagent Characteristics

RB5 dye (991.8 g mol^{-1}1; $\lambda_{max} = 596$ nm, Color Index 20505, purity of 98%) was supplied by Sigma-Aldrich (Brazil). The salt used to the modification of the CF was NH_4VO_3 (purity of 99.0%), which was supplied by Merck (Germany). Distilled water was used to prepare all solutions.

Preparation and Characterization of Modified Films

Chitosan was obtained from shrimp waste (*Penaeus brasiliensis*) according to the procedure developed by Moura et al. [25]. Deacetylation of chitin was carried out with sodium hydroxide solution (421 g L^{-1}) at 130 ± 1 °C, under constant agitation, and reaction time was of 4 h. Chitosan was purified by dissolution in acetic acid solution (1%). The solution was centrifuged for the removal of insoluble material. Total precipitation of chitosan occurred by addition of sodium hydroxide solution until pH 12.5, followed by neutralization until pH 7.0. The chitosan suspension was centrifuged for separation of the supernatant and, afterwards, the chitosan paste was dried in spouted bed [26]. Deacetylation degree was determined by potentiometric linear titration, and the chitosan molecular weight was measured by viscosimetric method using Mark–Houwink–Sakurada equation ($K = 1.8 \times 10^{-3}$ mL g^{-1} and $\alpha = 0.93$) [27].

CF were prepared by casting technique, as follows: 1.5 g (dry basis) of chitosan powder was dissolved in acetic acid solution 0.1 mol L^{-1} at 300 rpm using a magnetic stirrer (Marte, MAG-01H, Brazil), in room temperature for 120 min. Then, the film-forming solution was centrifuged (Fanem, 206BL, Brazil) at 5000×*g* for 15 min. A volume (50 mL) of the film-forming solution was poured into a plexiglass plate to keep constant the total amount of chitosan. The films were obtained by solvent evaporation in an oven with air circulation at 40 ± 2 °C for 24 h. Finally, the films samples were removed from plates and conditioned in desiccators prior to the use [28].

Preliminary assays in the CF using the vanadium salt solution for films modification were performed. The modified films were obtained by adsorption of vanadium ions, in batch mode, under agitation of 50 rpm at room temperature by 24 h. The vanadium salt solution concentration (NH_4VO_3) was of 100 mg L^{-1} [24]. The pH was adjusted to 3.0, in which the swelling degree of the films reaches values of approximately 300% [22], allowing that the ions diffuse into the CF. Finally, the ions were eluted using NH_4OH solution 0.01 mol L^{-1}. The preliminary tests showed that, the CVF presented suitable characteristics of tensile strength, elongation and thickness after the elution, and approximately 100% of the vanadate was eluted.

The tensile strength and the elongation of the CF and CVF were measured by a texture analyzer (Stable Micro Systems, TA-XT-2i, UK), with a 50 N load cell, according to ASTM [29]. The testing speed for texture analysis was of 2 mm s^{-1}. The thicknesses were measured by a digital micrometer (Insize, IP54, Brazil), with 0.0010 mm of resolution. The CF and CVF samples were analyzed by infrared with attenuated total reflectance (FTIR-ATR) (Prestige 21, the 210045, Japan) [30]. Differential scanning calorimetric analyses (DSC) were carried out with a heating rate of 10 °C min^{-1}, in the temperature range from 30 to 400 °C under N_2 at 50 mL min^{-1} (Shimadzu, DTG-60, Japan) [31]. X-ray diffraction analyses of the films were performed by a X-ray diffractometer (model D8 Advance, Brunker, Germany), with Cu Kα radiations [32]. The X-ray tube was operated at 40 kV and 40 mA. The diffraction results were obtained over a 2θ range from 5 to 70°, at a rate of 2° min^{-1} (2θ) and a step size of 0.02° (2θ). The films crystallinities were calculated by Eq. (1):

$$X_c = \frac{F_c}{F_c + F_a} 100\% \quad (1)$$

where X_c is the crystallinity, F_c is the diffraction peak area relevant to crystalline state structure, and F_a that correspond to the non-crystalline structure calculated from the diffraction patterns [32].

Adsorption Assays

The RB5 solutions (1.0 g L^{-1}) were prepared and, the pH values were adjusted at 4.0, 6.0 and 8.0, using buffer disodium phosphate/citric acid solution (0.1 mol L^{-1}). The adsorption assays using CVF were performed in three steps. Firstly, the pH effect (from 4.0 to 6.0) was evaluated at the temperature 298 K and 100 rpm for 24 h, with adsorbent dosage of 500 mg L^{-1} and the dye concentration (RB5) of 100 mg L^{-1}. In the second step, equilibrium isotherms were carried out at temperatures of 298, 308, 318 and 328 K, in the more suitable pH condition and with dye concentrations from 50 to 500 mg L^{-1}. In the third step, adsorption kinetic curves were performed at different stirring rates (50, 100, 200 and 300 rpm) and, the assays were carried out in the more suitable pH condition at room temperature. For all tests, the concentrations of RB5 solutions were measured by a spectrophotometer (Biospectro, SP-22, Brazil). Blanks were performed, and assays were carried out in two repetitions. The removal percentage ($R\,\%$), the amounts of RB5 adsorbed onto CVF at equilibrium (qe, mg g^{-1}) and at any time (q_t, mg g^{-1}) were calculated as follows (Eqs. 2–4):

$$R\% = \frac{(C_0 - C_e)}{C_0} 100 \tag{2}$$

$$q_e = \frac{V(C_0 - C_e)}{m} \tag{3}$$

$$q_t = \frac{V(C_0 - C_t)}{m} \tag{4}$$

where C_0 is the initial dye concentration (mg L^{-1}), C_e is the dye concentration at equilibrium (mg L^{-1}), C_t is the dye concentration at any time t (mg L^{-1}), V is the volume of dye solution (L) and m is the amount of adsorbent (g).

Equilibrium and Thermodynamic Data

The equilibrium data for the RB5 adsorption onto CVF were obtained at 298, 308, 318 and 328 K. Between the various adsorption equilibrium models in literature, the most used are of Langmuir (Eq. 5) and Freundlich (Eq. 6) isotherms [33], thus, the equilibrium data were fitted by these isotherms models.

$$q_e = \frac{q_m k_L C_e}{1 + (k_L C_e)} \tag{5}$$

$$q_e = k_F C_e^{1/nF} \tag{6}$$

where C_e is the equilibrium dye concentration in solution (mg L^{-1}), q_e is the equilibrium adsorption capacity (mg g^{-1}), q_m is the maximum adsorption capacity of the adsorbent (mg g^{-1}), K_L is the Langmuir constant (L mg^{-1}), k_F is the Freundlich constant [(mg g^{-1})(mg $L^{-1})^{-1/n}$] and $1/nF$ is the heterogeneity factor.

The Gibb free energy (ΔG^0) (kJ mol^{-1}), for the RB5 adsorption onto CVF was determined by Eq. (7). The enthalpy change (ΔH^0) (kJ mol^{-1}) and the entropy change (ΔS^0) (kJ mol^{-1} K^{-1}) were determined by Van't Hoff plot, according to Eq. (8) [34, 35].

$$\Delta G^0 = -RT \ln(\rho_w K_D) \tag{7}$$

$$\ln(\rho K_D) = \frac{\Delta S^0}{R} - \frac{\Delta H^0}{RT} \tag{8}$$

where K_D is the equilibrium constant (L mg^{-1}), ρ_w is the water density (mg L^{-1}), T is the temperature (K) and R is the gas universal constant (J mol^{-1} K) [36].

Kinetic Analysis

To investigate the adsorption kinetics, the models of pseudo-first order (Eq. 9), pseudo-second order (Eq. 10) and Elovich (11) were used to fit the experimental data [33, 37].

$$q_t = q_1(1 - \exp(-k_1 t)) \tag{9}$$

$$q_t = \frac{t}{(1/k_2 q_2^2) + (t/q_2)} \tag{10}$$

$$q_t = \frac{1}{a} \ln(1 + abt) \tag{11}$$

where k_1 (min^{-1}) and k_2 (g mg^{-1} min^{-1}) are the rate constants of the pseudo-first order and pseudo-second order models, respectively, q_1 and q_2 are the theoretical values for the adsorption capacity (mg g^{-1}), t is the time (min), a is the initial velocity due to dq/dt with $q_t = 0$ (mg g^{-1} min^{-1}) and b is the desorption constant of the Elovich model (g mg^{-1}).

Regression Analysis

Nonlinear regression to fit the equilibrium data and kinetic data was performed. The parameters were determined through Quasi-Newton estimation method by use of the Statistic 7 software (Statsoft, USA). The fits quality of the model was evaluated by coefficient of the determination (R^2) and average relative error (ARE) [38].

Desorption and Reuse

Desorption is an important operation to justify the applicability of an adsorbent [39]. Thus, desorption and reuse of the

CVF in the RB5 adsorption were evaluated to verify if the changes caused by the vanadate in the polymer were effective. Desorption assays were carried out in batch system at 298 K and 100 rpm. To identify the more appropriate eluent to remove the RB5 from the CVF, four solutions in two concentrations were tested: NaCl, EDTA, NaOH and NH_4OH (from 0.01 to 0.001 mol L^{-1}). After 24 h, the final concentrations of dye present in the solutions were determined for all eluents tested. Once determined the more suitable eluent, five cycles of adsorption/desorption were carried out, and the adsorption percentage and the desorption percentage were determined in each cycle.

Results and Discussion

CVF and CF Characteristics

Chitosan powder presented deacetylation degree of 95 ± 1% and average molecular weight of 150 ± 3 kDa, and these values are according to literature [40]. The CF and CVF were characterized by the tensile strength, elongation and thickness. For both films, the values were for tensile strength of 26.3 ± 2 MPa, elongation of 8.7 ± 1.3% and thickness of 64 ± 4 µm. Based on these results and in the literature, can be observed that CVF samples present interesting mechanical properties and are suitable for use in adsorption processes [28].

Figure 1 shows the FT-IR spectrums of CF and CVF. In Fig. 1a of CF spectrum, the characteristic bands of the chitosan were observed. The bands in the range 3350–3150 cm^{-1} are relative to the N–H and O–H stretching. Stretching vibrations of C=O relative to the amides were shown at 1650 cm^{-1}. At 1550 cm^{-1} N–H angular vibrations were observed, and in 1150 cm^{-1} the N–C stretching vibrations were identified. The bands 1410 and 1340 cm^{-1}, can be attributed to the CH_2 bend and CH_3CO stretching, respectively. The band in 1020 cm^{-1} can be assigned to the C–O stretching [41, 42]. In Fig. 1b, CVF spectrum shows the N–H and O–H stretching bands at 3350 cm^{-1}, and at 1640 cm^{-1} the stretching vibrations of C=O, similarly to the CF. However, at 1550 cm^{-1} a decrease in the N–H band, relative to the angular vibrations was observed. The CH_2 band at 1410 cm^{-1} relative to bending vibrations in Fig. 1a was not pronounced in the CVF spectrum (Fig. 1b). Besides, CH_3CO stretching at 1340 cm^{-1} and the band at 1020 cm^{-1} (assigned to the C–O stretching) were reduced drastically in the CVF. This can be due to the presence of vanadate in the CF, which led to a stabilization of the polymer functional groups, hindering the conversion of radiation into vibrational energy. It can be observed that, the angular vibrations suffered the major changes in their ability to absorb energy in the infrared.

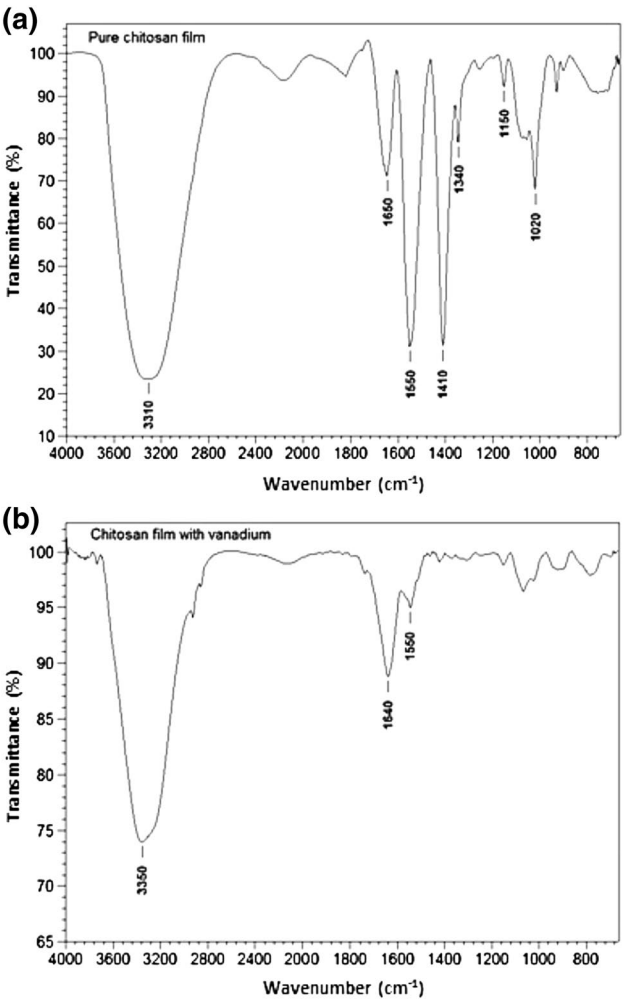

Fig. 1 FT-IR vibrational spectrums of the films samples: **a** CF, and **b** CVF

In Fig. 2 are shown the XRD curves of CF (Fig. 2a) and CVF (Fig. 2b). CF exhibited a series of crystalline peaks between 12° and 34° values of 2θ. The crystallinity of the CF was of 28%. XRD pattern of the CVF indicated a shape of typical amorphous structure. This shows that due to the vanadate presence, the polymeric structure was changed and, the crystalline zones disappeared. The vanadate presence in the polymer can to have weakened the hydrogen bonds between amino groups and hydroxyl groups in the CF, leading to interconnects of different polymer chains, resulting in an amorphous structure of the CVF [32, 43, 44].

In Fig. 3a, the DSC curve of CF showed the endothermic peak relative to the glass transition of the material at 60 °C. In this temperature, the polymer chains have increased its internal energy, enabling mobility and conformational change. After the glass transition, other endothermic change occurred at 90 °C, and this can be attributed to the loss of film surface water. Furthermore, at 281 °C, an exothermic

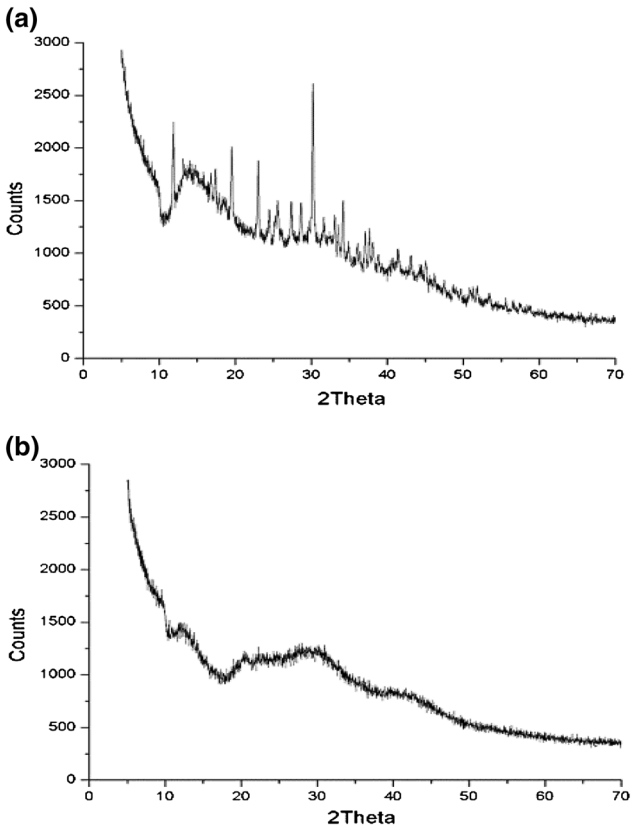

Fig. 2 X-ray diffraction (XRD) of the films samples: **a** CF, and **b** CVF

peak is attributed to the recrystallization of the polymer structure, with enthalpy of 53.6 J g^{-1}. At 328.4 °C, an endothermic peak with enthalpy of 29.9 J g^{-1} was observed. This behavior is characteristic to the semicrystalline polymers, and it is a thermodynamic change of first order (crystalline fusion). In this temperature, the energy is enough to overcome the secondary intermolecular forces between the crystalline phase chains, occurring a change in the polymer structure for a fluid state [45]. In Fig. 3b for the CVF, the DSC analysis showed that the band at 328.4 °C related to the crystalline fusion of CF, not appeared in the CVF. This change occurred due to the amorphous characteristic of the CVF, because amorphous polymers not present this energetic modification. This change can be attributed to the presence of vanadate in the polymer arrangement, which leads to a restructuration of the chitosan chains [46].

pH Effect in RB5 Adsorption onto CVF

In order to verify the pH effect in the RB5 adsorption capacity onto CVF, Fig. 4 presents the values of adsorption capacity and the removal percentage at different pH values. The RB5 adsorption was favored by pH decreases from 8.0 to 4.0. This behavior occurred because the H^+ ions in the solution increased the amino groups protonation (NH_2) of the chitosan, which were converted in NH_3^+ [47–49]. These protonated amine groups were responsible for interaction with the RB5 anionic dye. Thus, the most suitable condition for RB5 adsorption onto CVF was at pH 4.0. In this condition, the CVF presented adsorption capacity about 360 mg g^{-1} and removal percentage around 95%. Therefore, for the continuity of the work, it was used this pH value.

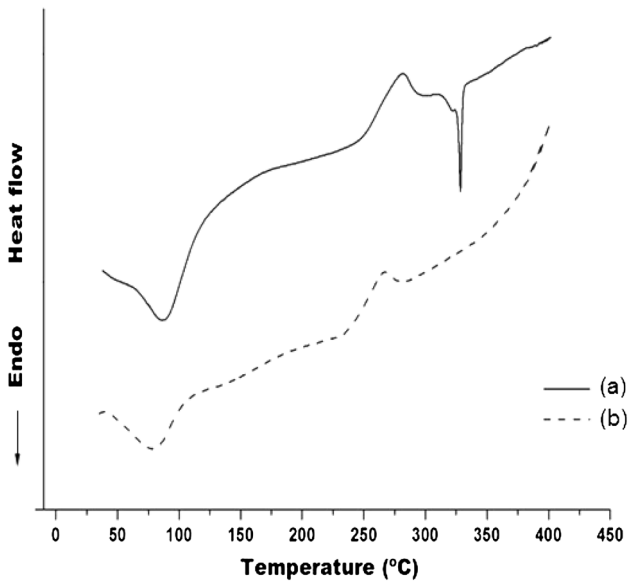

Fig. 3 Differential scanning calorimetry curves (DSC) of the films samples: (*a*) CF, and (*b*) CVF

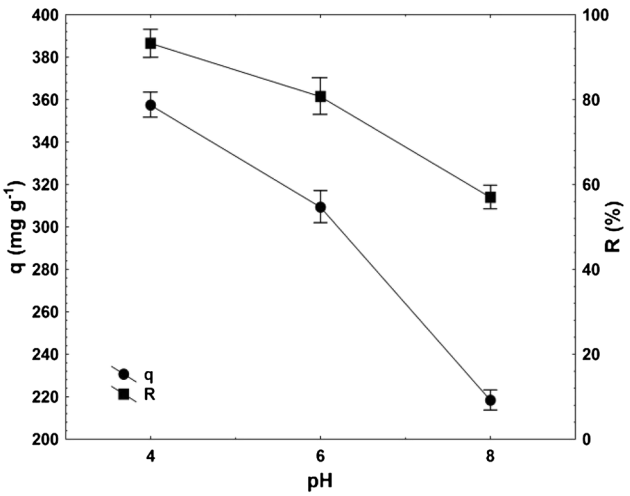

Fig. 4 Adsorption capacity (*q*) and removal percentage (*R*) for the RB5 adsorption by CVF at different pH values

Equilibrium and Thermodynamic Studies

The adsorption equilibrium curves at different temperatures (from 298 to 328 K) were carried out to determine the effect of temperature on adsorption capacity. These results are shown in Fig. 5. It was observed that the isotherms are characterized as type I [33]. The initial inclination shows the affinity between CVF and RB5, and the plateau represents the maximum adsorption capacity. Furthermore, the Fig. 5 shows that the adsorption capacity increased with the decreased of temperature, and the maximum values were obtained at 298 K. The equilibrium parameters for the RB5 adsorption onto CVF were determined by Langmuir and Freundlich models, which are presented in Table 1. Based on the values of coefficient of determination ($R^2 > 0.98$) and average relative error ($ARE < 5.00\%$), the Langmuir model was the more suitable to represent the equilibrium data and,

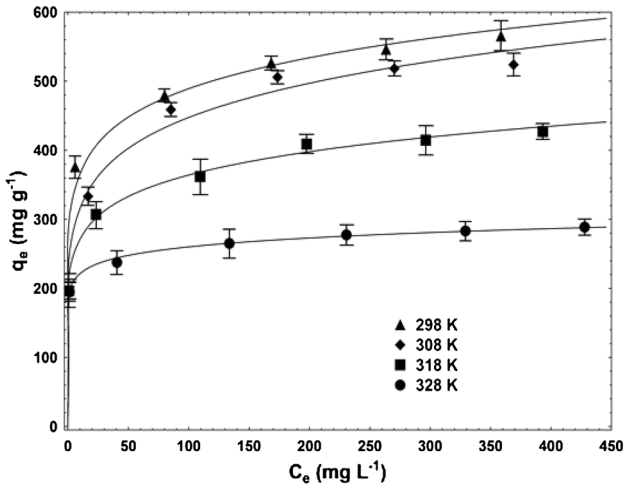

Fig. 5 Equilibrium curves for the RB5 adsorption by CVF at different temperatures

the q_m value was of 521.8 mg g^{-1} at 298 K. This behavior proposes that the dye adsorption occurred in a monolayer of the CVF. The interaction between adsorbent and adsorbate was electrostatic, due to the protonated amino groups of the CVF and the anionic sulfonated groups of the dye. Thus, when the protonated amino groups of the monolayer were compromised, there was not more how to continue the adsorption.

The thermodynamic equilibrium constant (K_D), the Gibbs free energy change (ΔG^0), the enthalpy change (ΔH^0) and the entropy change (ΔS^0) were estimated. The K_D values increased with the decrease temperature (from 188 to 273 L g^{-1}), showing that the adsorption operation was favored in all temperatures. The negative values of ΔG^0 (from −31.0 to −33.1 kJ mol^{-1}) indicated that the adsorption was energetically favorable. The negative value of ΔH^0 (−9.91 kJ mol^{-1}) showed an exothermic process, and its low value confirmed an electrostatic interaction between adsorbent and adsorbate [50]. The value of ΔS^0 was positive (0.0705 kJ mol^{-1} K^{-1}), suggesting an increase in randomness at the solid/solution interface [51]. Thus, both thermodynamic parameters contributed to favoring the adsorption and for the negatives values of ΔG^0.

Kinetic Studies

The adsorption kinetic data for the RB5 onto CVF were obtained at pH 4.0 and temperature of 298 K. The stirring rate effect was verified in different conditions (from 50 to 300 rpm), and the curves are presented in Fig. 6. The adsorption rate increased with the increase of stirring rate. Pseudo-first order, pseudo-second order and Elovich models were fitted to the experimental data. In the kinetics profiles were observed that, in around 80 min occurred a reduction in the adsorption rates, thus, can to have occurred a change in the mass transfer mechanism. After this, the adsorption rates

Table 1 Isotherm parameters for the RB5 adsorption onto chitosan-vanadate film at different temperatures

Temperature (K)	Langmuir			
	k_L (L mg^{-1})	q_m (mg g^{-1})	R^2	*ARE* (%)
298	1.92	521.8	0.998	4.09
308	0.91	499.8	0.981	3.34
318	0.96	397.4	0.986	4.43
328	1.90	259.9	0.999	1.70
Temperature (K)	Freundlich			
	k_F (mg g^{-1}) (mg L^{-1})$^{-1/nF}$	n_F	R^2	*ARE* (%)
298	273.10	7.5	0.988	6.31
308	222.74	6.1	0.971	5.24
318	201.76	7.0	0.951	10.30
328	188.47	12.9	0.975	4.93

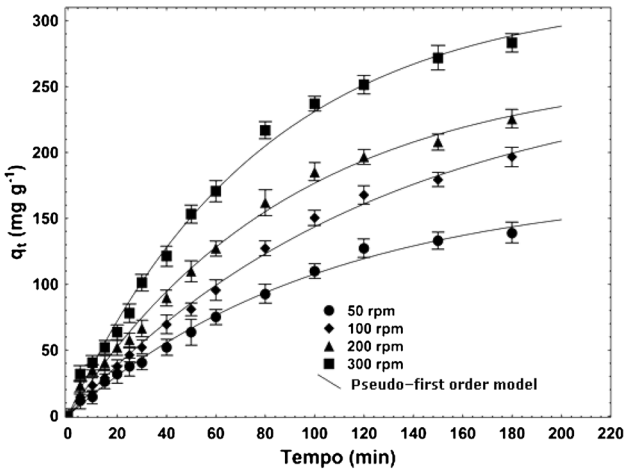

Fig. 6 Stirring rate effect for the RB5 adsorption by CVF at different conditions

were controlled by the internal mass transfer. Based on the values of coefficient of determination ($R^2 > 0.99$) and average relative error ($ARE < 5.00$), the pseudo-first order model was the more suitable to represent the adsorption kinetics.

Desorption and Reuse

The desorption operation of RB5 from the CVF was evaluated by four solutions (NaCl, EDTA, NaOH and NH_4OH), at different concentrations (0.01–0.001 mol L^{-1}). Table 2 shows the values of desorption percentages found in each treatment and, can be observed that the NH_4OH 0.01 mol L^{-1} was the most suitable eluent. The presence of this eluent resulted in an elevation of the pH value and, consequently, the deprotonation of the amino groups. This led to the removal of the anionic dye from the chitosan polymer chain. It can be inferred that the results corroborated with the electrostatic interaction mechanism, since desorption occurred in all conditions studied, showing a low energy involved in the regeneration.

Table 2 Results for RB5 desorption from CVF with different eluents

Eluents	Concentration (mol L^{-1})	Desorption (%)
NaOH	0.001	71.7 ± 2.4
	0.01	92.1 ± 1.6
NH_4OH	0.001	89.5 ± 1.2
	0.01	95.9 ± 1.4
NaCl	0.001	41.2 ± 1.4
	0.01	52.1 ± 1.9
EDTA	0.001	30.7 ± 2.6
	0.01	42.1 ± 1.9

After setting the appropriate eluent, five cycles of adsorption/desorption were performed to evaluate if the CVF could be reused. Figure 7 shows the percentage removal values in different cycles of adsorption/regeneration. It can be seen from Fig. 7 that the CVF presented a good performance in the reuse, because after five cycles of adsorption/desorption, the CVF showed its adsorption capacity reduced only about 20%.

Conclusion

The modification of CF by vanadium ions for use as adsorbent of RB5 in aqueous solution was investigated, to improve its the regeneration capacity. The CVF showed suitable mechanical properties. The FT-IR spectrum of chitosan-vanadate film showed changes in the characteristics bands relative to the CF. XRD pattern of the CF showed a change from semicrystalline to amorphous shape. The DSC of chitosan-vanadate film presented a reduction in the enthalpy of the glass transition, and the thermal degradation not occurred with the modification, which was favored at pH of 4.0. The Langmuir model represented the system equilibrium, being the maximum adsorption capacity was of 522 mg g^{-1} at 298 K, and the adsorption was exothermic. The pseudo-first order model was that best fitted the adsorption kinetics data. The most appropriate eluent was NH_4OH 0.01 kg mol L^{-1} and, five cycles of adsorption/desorption were possible.

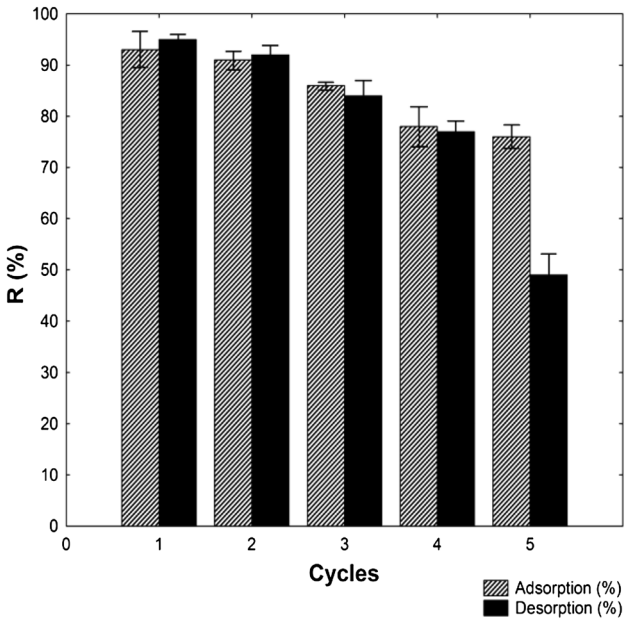

Fig. 7 Percentage removal in different cycles of adsorption/regeneration for RB5 from CVF

Acknowledgements The authors thank CAPES/Brazil (Coordination for the Improvement of Higher Education Personnel) and CNPq/Brazil (National Council for Scientific and Technological Development) for the financial support. The authors too thank CEME-SUL/FURG/Brazil (Electron Microscopy Center of South/Federal University of Rio Grande/RS/Brazil) due to the microscopy images.

References

1. Ahmad MZ, Rahman NK (2011) Chem Eng J 170:154
2. Ali I, Aboul-Enein HY (2006) Instrumental methods in metal ions speciation: chromatography, capillary electrophoresis and electrochemistry, Taylor & Francis Ltd., New York
3. Ali I, Aboul-Enein HY, Gupta VK (2009) Nano chromatography and capillary electrophoresis: pharmaceutical and environmental analyses. Wiley, Hoboken
4. Khan TA, Sharma S, Ali I (2011) J Toxicol Environ Health Sci 10:286
5. Crini G, Badot PM (2008) Prog Polym Sci 33:399
6. Cheng JS, Du J, Zhu W (2012) Carbohydr Polym 88:61
7. Wan M, Kan C, Rogel BD, Dalida MLP (2010) Carbohydr Polym 80:891
8. Wan Ngah WS, Teong LC, Hanafiah MAKM. (2011) Carbohydr Polym 83:1446
9. Reddy MCS, Sivaramakrishna L, Reddy AV (2012) J Hazard Mater 203–204:118
10. Ali I, Gupta VK (2006) Nat Protoc 1:2661
11. Ali I (2012) Chem Rev 112:5073
12. Ali I (2010) Sep Purif Rev 39:95
13. Ali I, Asim M, Khan TA (2012) J Environ Manag 113:170
14. Ali I (2014) Sep Purif Rev 43:175
15. Muzzarelli RAA, Boudrant J, Meyer D, Manno N, DeMarchis M, Paoletti MG (2012) Carbohydr Polym 87:995
16. Ali I, Al-Othman ZA, Alwarthan A (2017) J Mol Liq 236:205
17. Ali I, Al-Othman ZA, Alwarthan A (2016) J Mol Liq 224:171
18. Ali I, Al-Othman ZA, Alwarthan A (2016) J Mol Liq 221:1168
19. Ali I, Al-Othman ZA, Alwarthan A (2016) J Mol Liq 219:858
20. Ali I, Al-Othman ZA, Alharbi OML (2016) J Mol Liq 218:465
21. Vieira RS, Oliveira MLM, Guibal E, Rodríguez–Castellón E, Beppu MM (2011) Coll Surf A 374:108
22. Rêgo TV, Cadaval TRS Jr, Dotto GL, Pinto LAA (2013) J Coll Interface Sci 411:27
23. Singh V, Pandey S, Singh SK, Sanghi R (2008) Sol-Gel Sci Technol 47:58
24. Cadaval TRS Jr, Dotto GL, Seus ER, Mirlean N, Pinto LAA (2015) Desalin Water Treat 57:16583
25. Moura CM, Moura JM, Soares NM, Pinto LAA (2011) Chem Eng Process 50:351
26. Dotto GL, Souza VC, Moura JM, Moura CM, Pinto LAA (2011) Dry Technol 29:1784
27. Weska RF, Moura JM, Batista LM, Rizzi J, Pinto LAA (2007) J Food Eng 80:749
28. Dotto GL, Moura JM, Cadaval TRS, Pinto LAA (2013) Chem Eng J 214:8
29. ASTM (2000) Standard test methods for tensile properties of thin plastic sheeting. Standard D882-02, Annual book of ASTM, pp 162–170
30. Silverstein RM, Webster FX, Kiemle DJ (2007) Spectrometric identification of organic compounds. Wiley, New York
31. Rivero S, García MA, Pinotti A (2010) Innov Food Sci EmergTechnol 11:369
32. Cheng M, Deng J, Yang F, Gong Y, Zhao N, Zhang X (2003) Biomaterials 24:2871
33. Ruthven DM (1984) Principles of adsorption and adsorption process. Wiley, New York
34. Liu Y (2009) J Chem Eng Data 54:1981
35. Esquerdo VM, Cadaval TRS Jr, Dotto GL, Pinto LAA (2014) J Colloid Interface Sci 424:7
36. Li W, Qi L, Aiqin W (2010) Polym Bull 65:961
37. Dotto GL, Pinto LAA (2011) J Hazard Mater 187:164
38. Martinez JM (2000) J Comput Appl Math 124:97
39. Guibal E (2004) Sep Purif Technol 38:43
40. Moura JM, Farias BS, Rodrigues DAS, Moura CM, Dotto GL, Pinto LAA (2015) J Polym Environ 23:470
41. Maji TK, Baruah I, Dube S, Hussain MR (2007) Bioresour Technol 98:840
42. Cui L, Jia J, Guo Y, Liu Y, Zhu P (2014) Carbohydr Polym 99:31
43. Liu Z, Ge X, Lu Y, Dong S, Zhao Y, Zeng M (2012) Food Hydrocolloid 26:311
44. Dotto GL, Cunha JM, Calgaro CO, Tanabe EH, Bertuol DA (2015) J Hazard Mater 295:29
45. Kousksou T, Jamil A, El Omari K, Zeraouli Y, Le Guer Y (2011) Thermochim Acta 519:59
46. Homer S, Kelly M, Day L (2014) Carbohydr Polym 108:1
47. Wu FC, Tseng RL, Juang RS (2000) J Hazard Mater B73:63
48. Guzmán J, Saucedo I, Navarro R, Revilla J, Guibal E (2002) Langmuir 18:1567
49. Cadaval TRS Jr, Camara AS, Dotto GL, Pinto LAA (2013) Desalin WaterTreat 51:7690
50. Machado FM, Bergmann CP, Lima EC, Royer B, Souza FE, Jauris IM, Calvete T, Fagan SB (2012) Chem Phys 14:11139
51. Bakhtiari N, Azizian S (2015) J Mol Liq 206:114